Chapter 3

Effect of 80 MeV O^{6+} ions on Organometallics Dispersed Polymer Films

Abstract

In this chapter effects of 80 MeV, O^{6+} ions were studied on ferric oxalate dispersed PMMA and PVC and Nickel dimethylglyoxime (Ni-DMG) dispersed PMMA films at different fluences. The results obtained from different characterization techniques showing the fluence dependent modification of above polymer composites. The radiation induced modifications in dielectric properties, microhardness, Mossbauer studies, surface morphology and average surface roughness of polymer composite films have been investigated at different concentrations (i.e. 5%, 10% and 15%) of filler and at different fluences.

3.0 Introduction

Metallized polymers now a day are of considerable technological importance and are used in a number of fields such as data storage, microelectronics, and packaging industry [1] The interaction between metals and polymers is generally very weak'and the cohesive energy of polymer is typically two orders of magnitude lower than the cohesive energy of metals [2]. During the last few years much work has been performed to study the different aspects of metal/polymer interface formation using various microscopic and surface sensitive techniques It is known that good adhesion between polymer and metal is crucial to device performance and reliability by the use of ion beams [3, 4].

Our interest in dispersion of organometallic compound is mainly because of ion irradiation induced enhancement of both electrical conductivity and mechanical hardness of polymers. In this study, we have synthesized three types of composites, their preparation, irradiation details and characterization techniques were discussed in article 2.3 and 2.4 respectively of Chapter 2.

Following three sets of composites were taken under study

3.1 Ferric oxalate dispersed PMMA films

3.2 Ferric oxalate dispersed PVC films

3.3 Ni-DMG dispersed PMMA films

Above polymer composites sets were irradiated with 80 MeV O^{6+} ions at a fluence of 1×10^{11} ions/cm^2 and 1×10^{12} ions/cm^2. We have studied the electrical, mechanical (i.e. microhardness) properties and surface roughness by means of LCR meter, Vickers' microhardness indentation, atomic force microscopy (AFM), respectively [5, 6, 7, 8, 9].

Mossbuer studies were carried out for 10% ferric oxalate dispersed PMMA pristine and irradiated films [10].

3.1 Ferric oxalate Dispersed PMMA Films

3.1 Results and Discussion

3.1.1 AC Electrical Frequency Response

3.1.1 (a) Conductivity vs frequency

AC electrical measurement was performed for pristine and irradiated samples. The resistance, capacitance and dielectric loss measurements were carried out over the frequency range 50 kHz to 10 MHz at ambient temperature. AC conductivity was calculated using equation 2 5 discussed in article 2 4.1 of Chapter 2. Fig.3.1 (a, b) shows the variation of conductivity with frequency for the pristine and irradiated samples at different ferric oxalate concentration. A sharp increase in conductivity was observed around 100 kHz for pristine and irradiated samples. It is also observed that conductivity increases with increasing concentration of dispersed ferric oxalate compound. For irradiated ferric oxalate at the fluence of 1×10^{11} ions/cm^2, further increase in conductivity is observed. The increase in conductivity with different ferric oxalate concentration for pristine samples may be attributed to the conductive phase formed by dispersed organometallic compound in polymer matrix.

It is known that electrical conductivity of such composites depends on the type and concentration of the dispersed compound [11, 12]. As a result the conductivity of dispersed films increases with increasing the concentration of ferric oxalate compound in the polymer matrix. It is also observed that after the irradiation the conductivity increases with increasing concentration of dispersed organometallic compound. It is expected that

ion irradiation promote the metal to polymer bonding and convert the polymeric structure in to hydrogen depleted carbon network. It is this carbon network that is believed to make the polymers more conductive [3].

3.1.1 (b) Dielectric constant vs frequency

The dielectric constant was calculated using formula 2.8 as discussed in article 2.4.1 of Chapter 2.The dielectric constant is studied with respect to the frequency at different concentration of ferric oxalate for pristine and irradiated (at a fluence of $1x10^{11}$ ions/cm^2) samples.

Fig. 3.2 shows that the dielectric constant remains almost constant up to 100 kHz. At these frequencies, the motion of the free charge carriers is constant and so the dielectric constant presumably remains unchanged. It is also observed that dielectric constant increases for irradiated films with fluence. The increase in dielectric constant may be attributed to the chain scission and as a result the increase in the number of free radicals, etc.

As frequencies increases further (i e. beyond 100 kHz), the charge carriers migrate through the dielectric and get trapped against a defect sites and induced an opposite charge in its vicinity. At these frequencies, the polarization of trapped and bound charges can not take place and hence the dielectric constant decreases [13].

The dielectric constant decreases at higher frequencies (i.e. beyond 100 kHz) and obeys the Universal law [14] of dielectric response given by $\varepsilon \alpha f^{n-1}$, where n is power law exponent and varies form zero to one ($0<n<1$), n=0.78 for pure PMMA, 0.84 for 5% dispersed ferric oxalate, 0.85 for 10%, and 15% dispersed ferric oxalate pristine films. The value of n=0.85 for pure PMMA, 5%, 10% and 15% ferric oxalate dispersed PMMA

films were obtained at the fluence of 1×10^{11} ions/cm^2 (Fig.3.2b) respectively The Fig. 3.2 (a, b) clearly shows that the frequency dependence of dielectric constant, ε, obeys Universal law. The observed nature of the fluence dependence of dielectric constant in studied frequency range can be explained by the prevailing influence of the enhanced free carriers due to the irradiation [15].

3.1.1 (c) Dielectric loss vs frequency

The dielectric loss is studied with respect to frequency at different concentration of ferric oxalate for pristine and irradiated (at a fluence of $1x10^{11}$ ions/cm^2) samples

Fig.3.3 (a, b) shows the variation of dielectric loss with frequency for pristine and irradiated samples of pure PMMA and ferric oxalate dispersed PMMA films at the concentration of 5%, 10% and 15% respectively.

It reveals that dielectric loss decreases exponentially as frequency increases. It is also observed that loss factor (tanδ) increases as concentration of ferric oxalate increases. Further moderate increase in tanδ occurs due to the irradiation. The growth in tanδ as increase in the conductivity is brought about by an increase in the conduction of residual current and the conduction of absorbance current [16].

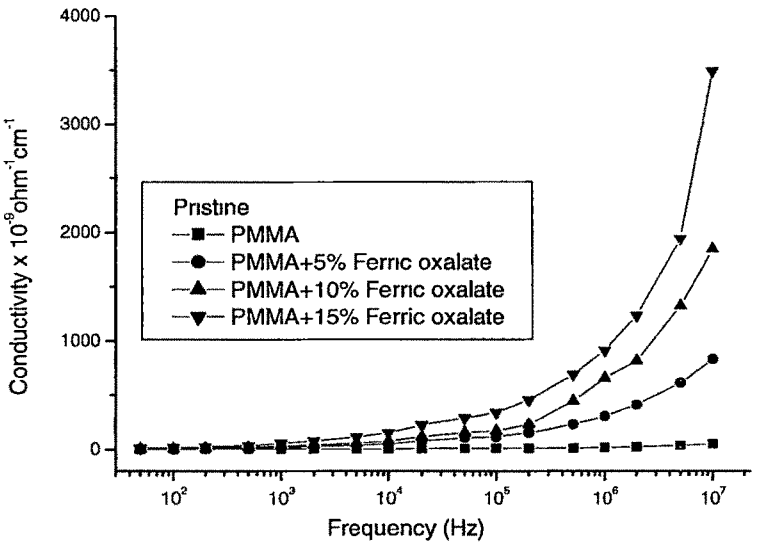

Figure 3.1(a) AC conductivity versus frequency for pristine pure and dispersed ferric oxalate in PMMA films.

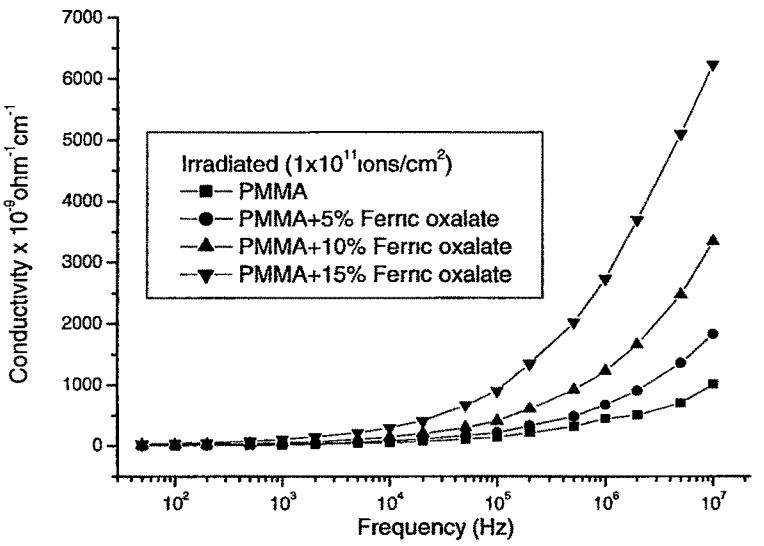

Figure 3.1(b) AC conductivity versus frequency for irradiated pure and dispersed ferric oxalate in PMMA films.

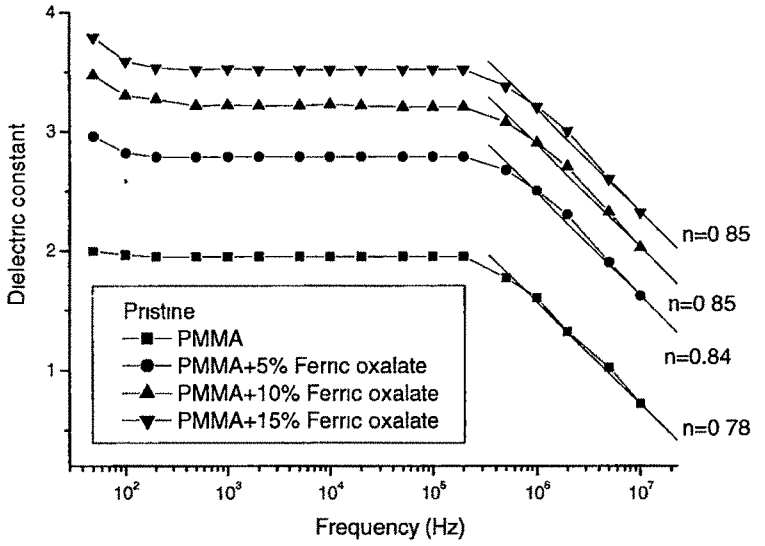

Figure 3.2(a) Dielectric constant versus frequency for pristine pure and dispersed ferric oxalate in PMMA films.

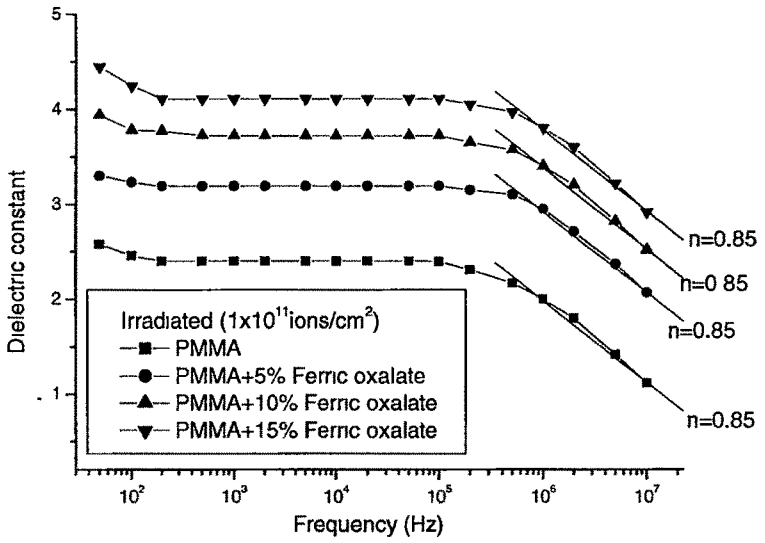

Figure 3.2(b) Dielectric constant versus frequency for irradiated pure and dispersed ferric oxalate in PMMA films.

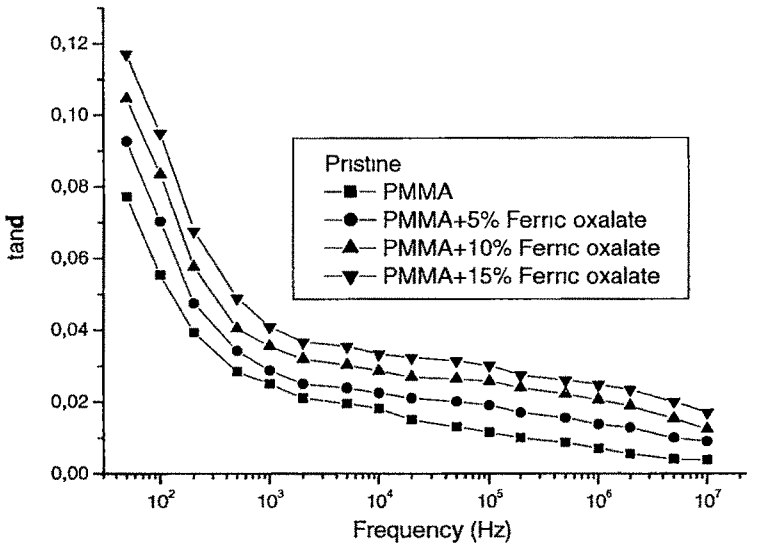

Figure 3.3(a) Dielectric loss versus frequency for pristine pure and dispersed ferric oxalate in PMMA films.

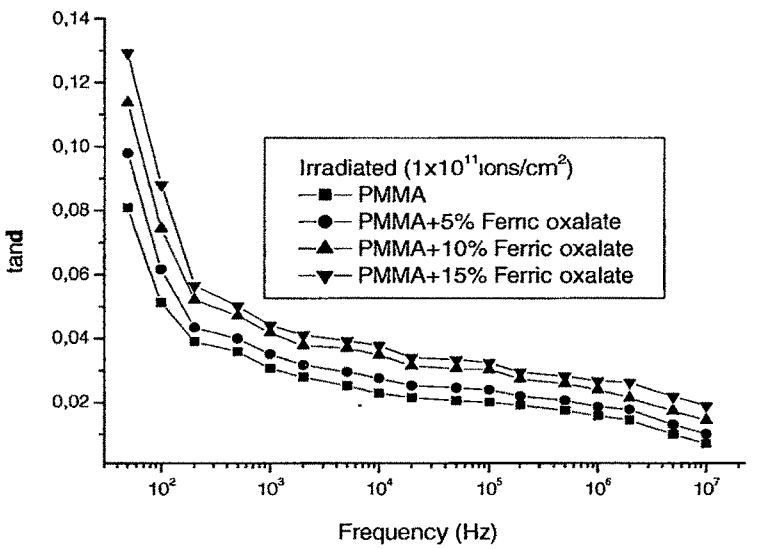

Figure 3.3(b) Dielectric loss versus frequency for irradiated pure and dispersed ferric oxalate in PMMA films.

3.1.2 Microhardness

The Vicker's microhardness of all the samples have been studied from the load range 50 mN to 1000 mN, and calculated using formula (equation) 2 10 given in article 2.4.2 of Chapter 2.

Fig.3.4 shows the plot of the Vickers' microhardness (H_v) versus applied load (P) for pristine and irradiated films of pure PMMA, and dispersed ferric oxalate compound of 5%, 10% and 15% in PMMA. The microhardness indentations were carried out on the surface of the pristine and irradiated films at room temperature under the different applied loads from 50 mN to 1000 mN and at a constant loading time of 30 seconds. It has been observed that microhardness (H_v) value increases with the load up to 100mN and then decreases and become saturated beyond the load of 400mN. Hardness can be defined as resistance to indenter penetration, or as the average pressure under the indenter, calculated as the applied load divided by the projected area of contact incorporating the plastic component of displacement. The hardness is known to be influenced by surface effects. Particularly at low penetration depths, the strain hardening modifies the true hardness of the material. Beyond certain load the polymer exhausts its strain hardening capacity and hardness tends to become constant. The rate of strain hardening is greater at low loads and decreases at higher loads [17, 18]. At the higher loads, beyond 400 mN, the interior of the bulk specimen is devoid of surface effects. Hence the hardness value at higher loads represents the true value of the bulk and it is consequently independent of the load. It is found that hardness increases as ferric oxalate concentration increases. It may be due to the improvement in bonding properties [19].

The hardness also increases on irradiation of the samples This may be attributed to hydrogen depleted carbon network which makes polymer harder [3].

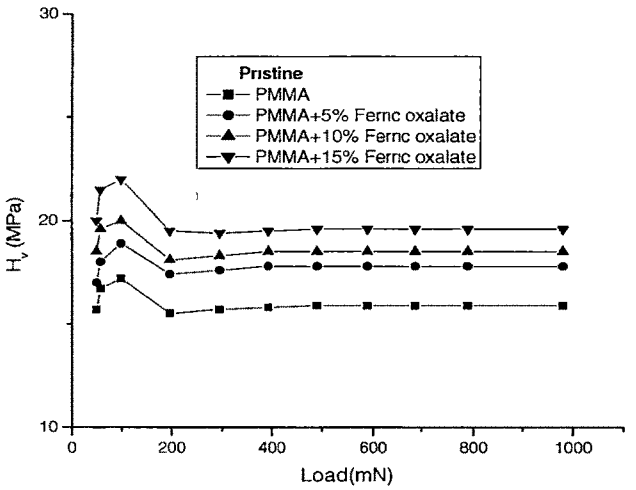

Figure 3.4(a) Plot of hardness (H_v) versus applied load (P) for pristine pure and dispersed ferric oxalate in PMMA films.

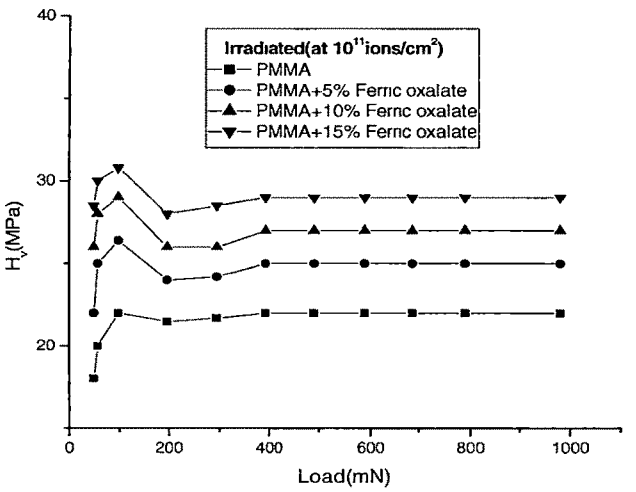

Figure 3.4(b) Plot of hardness (H_v) versus applied load (P) for irradiated pure and dispersed ferric oxalate in PMMA films.

3.1.3 Surface Morphology

The surface morphology of pristine and irradiated films of pure PMMA, and dispersed ferric oxalate compound of 10% and 15% in PMMA was measured by AFM on $2\times2\mu m^2$ area are shown in Fig3.5. Each AFM image was analyzed in terms of surface average roughness (Ra). The roughness values are 13nm, 21nm, and 26nm for pristine and 6nm, 19.2nm, and 19.52nm for irradiated (at a fluence of 10^{11} ions/cm^2) samples respectively.

It is found that roughness increases as ferric oxalate concentration increases. The increase in roughness may be due to the increase of density and size of metal particles on the surfaces of the PMMA films [20]. It is also observed that after irradiation the roughness of the surface decreases and the surface becomes significantly smoother. This relative smoothness is probably due to defect enhanced surface diffusion [21, 22].

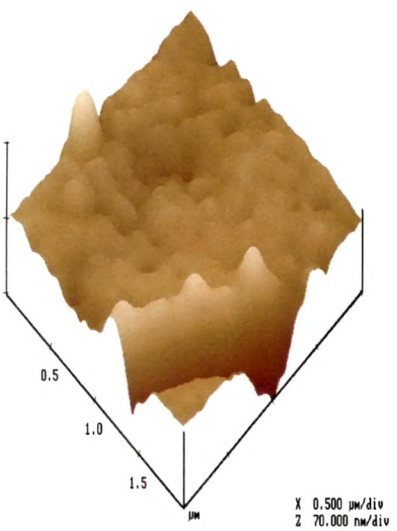

3.5(a)

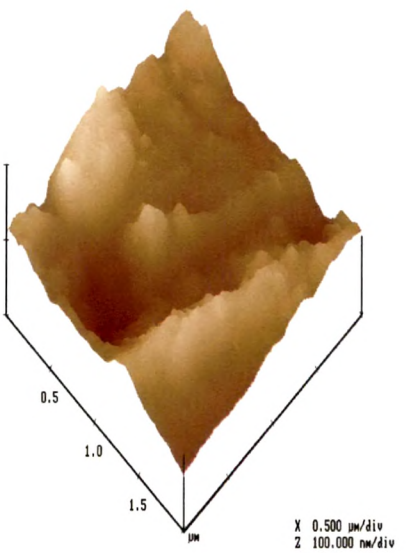

3.5(b)

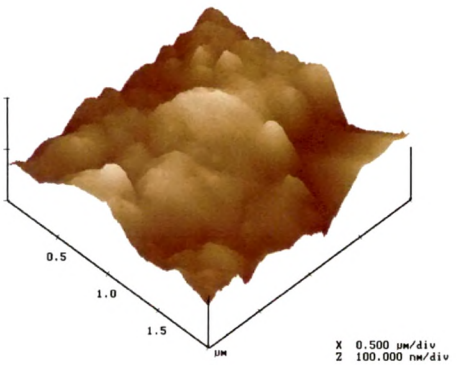

3.5(c)

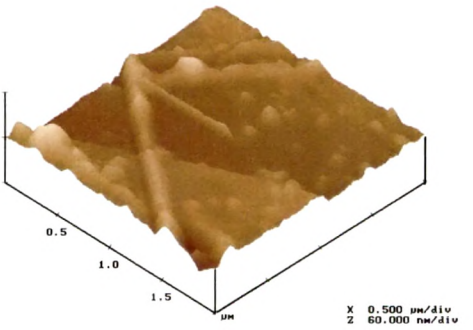

3.5(d)

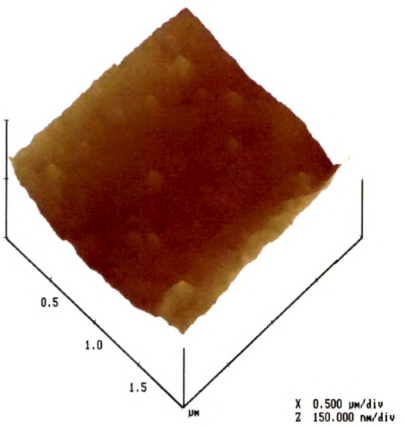

3.5(e)

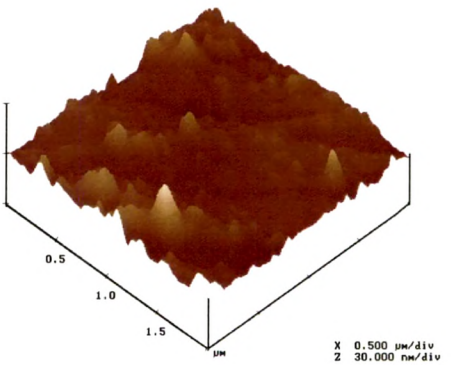

3.5(f)

Figure 3.5 (a) AFM image of pure PMMA film (pristine) (b) dispersed ferric oxalate (10%) in PMMA film (pristine) (c) dispersed ferric oxalate (15%) in PMMA film (pristine) (d) pure PMMA film (irradiated) (e) dispersed ferric oxalate (10%) in PMMA film (irradiated) (f) dispersed ferric oxalate (15%) in PMMA film (irradiated).

3.1.4 Mossbauer Studies

Mossbauer spectra were recorded for 10% ferric oxalate dispersed PMMA samples before and after irradiation. The least square fitted values of unirradiated sample are listed in Table 3.1. The fitted values indicate quadrupole splitting (QS) of ~0.45 mm/sec which corresponds to the Fe-C complex as reported earlier [23]. Thus in unirradiated sample there is only Fe-C non-magnetic complexes formed. It is possible that Fe ions were either residing in the voids between the chains or got attached to the $-COOCH_3$ group in the side chain without cross linking before irradiation. PMMA is known to undergo chain scissioning even at low (KeV) ion energies. Therefore high energy of the ion transferred energy per atom to the polymer chains makes scissioning more intense which may result in the amorphization of the sample. In the present case, after high energy irradiation of ferric oxalate dispersed PMMA films, it is expected that there is a possibility of the formation of cluster of Fe with oxygen, giving rise to magnetic interaction. However, the irradiated sample showed magnetic site with field values of ~ 510 KOe.

This indicates that there is a formation of Fe-O (could be Fe_2O_3 phase) complex in to the polymer matrix, by consequently breakage of Fe-C bonds which were observed in unirradiated sample. From Mossbauer spectra, the value of the QS and isomer shift (IS) for the irradiated samples showed that Fe is in the state 3+ or more. The spectra indicate the formation of magnetic sextet (Fe-O) with a doublet (Fe-C). The % of absorption was low due to less quantity of irradiated material.

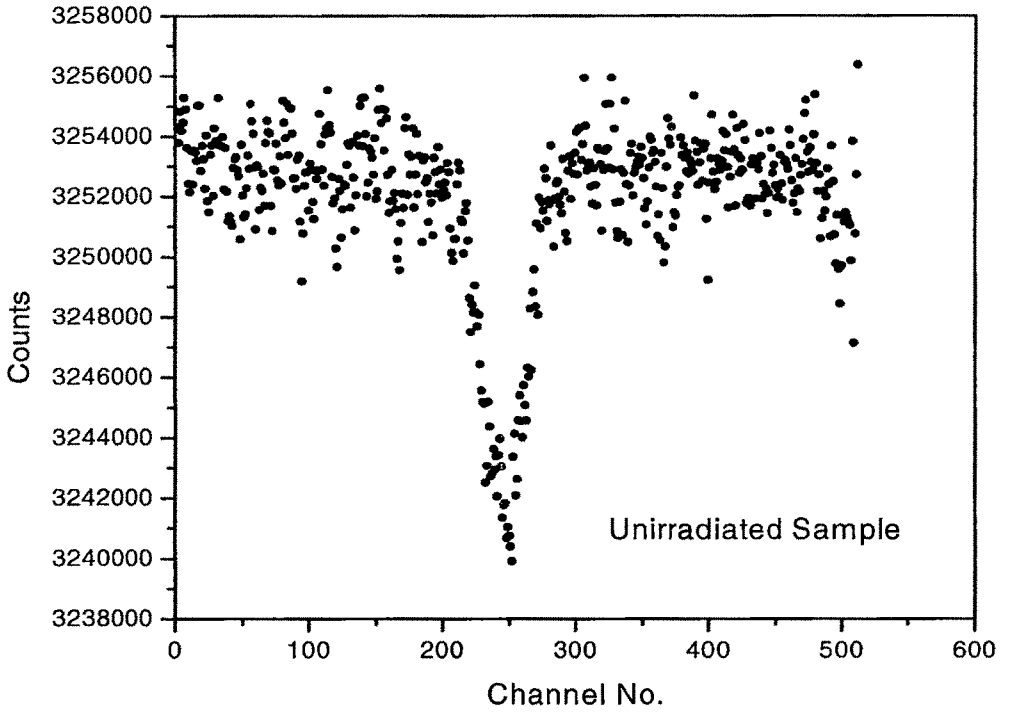

Figure 3.6(a) Mossbauer spectra of dispersed ferric oxalate (10%) in PMMA film (pristine).

Table-3.1: Mossbauer parameter of dispersed ferric oxalate (10%) in PMMA film.

Quadrupole splitting (mm/sec)	Isomer Shift (mm/sec)	Fractional Area
0.45	-0.29	1.00

3.1.5 Conclusion

Ion irradiation has been shown to significantly enhance both electrical and micro hardness of organometallic compound dispersed PMMA films. It may be attributed to (i) metal to polymer bonding and (ii) conversion of the polymeric structure in to hydrogen depleted carbon network. Thus irradiation makes the polymer harder, more conductive. It is also observed that dielectric constant obeys Universal law of dielectric response. The surface roughness increases as ferric oxalate concentration increases and decreases on irradiation as observed from AFM studies. Mossbauer studies indicate that there is a formation of Fe-O (could be Fe_2O_3 phase) complex in to the polymer matrix due to the irradiation.

3.2 Ferric oxalate Dispersed PVC Films

3.2 Results and Discussion

3.2.1 AC Electrical Frequency Response

3.2.1 (a) Condcutivity vs frequency

The conductivity was calculated using the relation $\sigma=t/R\ A$ ($\Omega^{-1}cm^{-1}$), where R is the resistance measured, A is the cross-sectional area of the electrode and t is the thickness of the polymeric film as discussed in article 2.4.1 of Chapter 2 and plotted with respect to frequency keeping fluence constant.

AC electrical measurement was performed for pristine and irradiated samples. Fig.3.7 (a, b and c) shows the variation of conductivity with frequency for the pristine and irradiated samples at different ferric oxalate concentration. A sharp increase in conductivity was observed around 100kHz in pristine as well as irradiated samples. It was also observed that conductivity increases with increasing concentration of dispersed ferric oxalate compound (Fig.3.7a, pristine) as well as those irradiated at the fluence of $1x\ 10^{11}$ ions/cm^2 (Fig.3.7b) and $1x\ 10^{12}$ ions/cm^2 (Fig.3.7c) respectively. The increase in conductivity with different ferric oxalate concentration for pristine samples may be attributed to the conductive phase formed by dispersed organometallic compound in polymer matrix. It is known that electrical conductivity of such composites depends on the type and concentration of the dispersed compound [11, 12]. As a result the conductivity of dispersed films increases with increasing the concentration of ferric oxalate compound in the polymer matrix. It is also observed that after the irradiation the conductivity increases with fluence (Fig.3.7). Irradiation is expected to promote the metal to polymer bonding and convert the polymeric structure in to hydrogen depleted carbon

network. It is this carbon network that is believed to make the polymers more conductive [3].

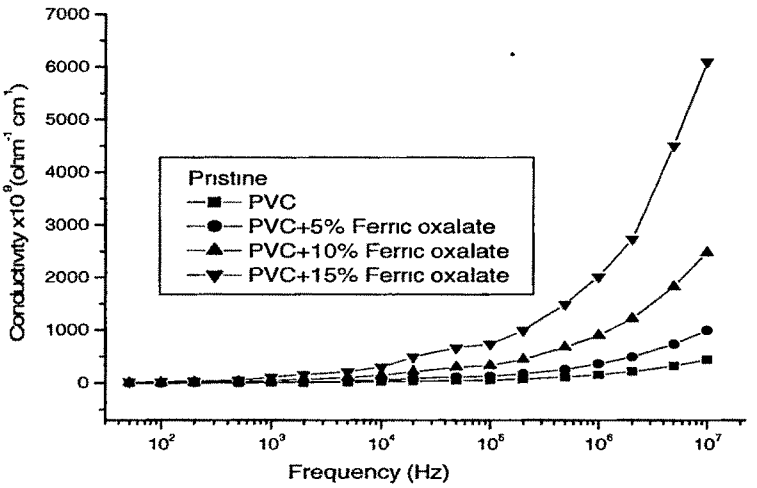

Figure 3.7(a) AC conductivity versus frequency for pristine pure and dispersed ferric oxalate in PVC films.

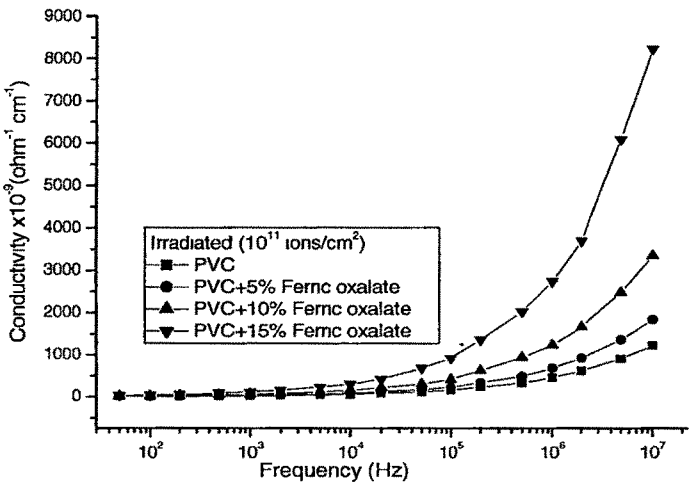

Figure 3.7(b) AC conductivity versus frequency for irradiated (at the fluence of 1x 10^{11} ions/cm^{2}) pure and dispersed ferric oxalate compound in PVC films.

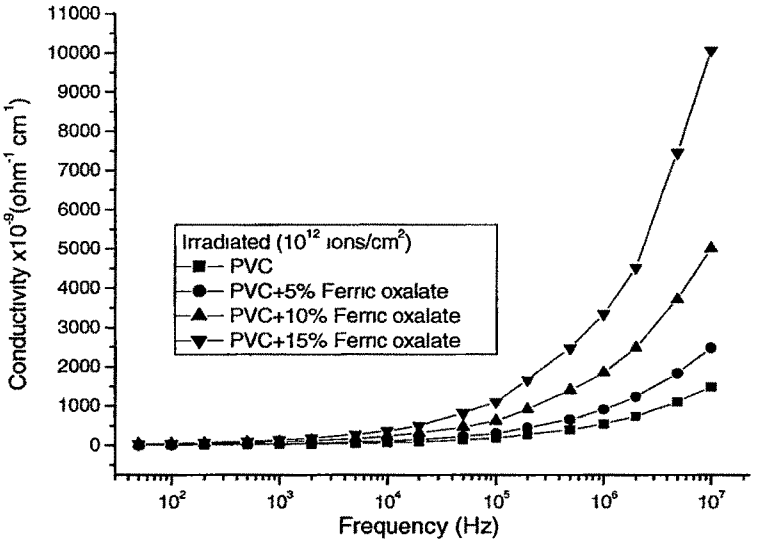

Figure 3.7(c) AC conductivity versus frequency for irradiated (at the fluence of 1x 10^{12} ions/cm^2) pure and dispersed ferric oxalate compound in PVC films.

3.2.1 (b) Dielectric constant vs frequency

Dielectric constant was calculated using formula 2.8 as given in article 2.4.1 of Chapter 2. Fig 3.8(a, b and c) shows the plot of dielectric constant versus frequency for pristine and irradiated samples of pure PVC and different concentration of ferric oxalate dispersed PVC films. When the fillers are dispersed in the insulating polymer, the dielectric constant of composites investigated increases with concentration of filler. Such results have been observed experimentally [24, 25].The partial agglomerations also increase with increasing the filler concentration as shown in Fig.3.11 (AFM).

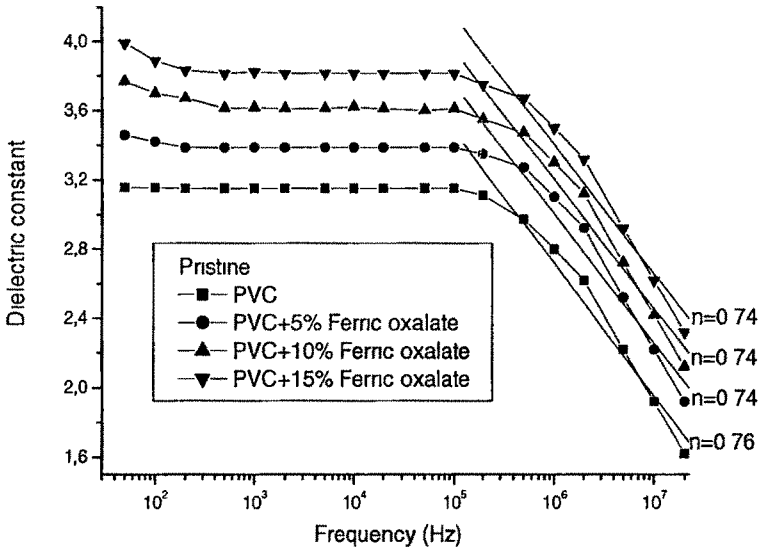

Figure 3.8(a) Plot of dielectric constant versus frequency for pristine pure and Dispersed ferric oxalate compound in PVC films.

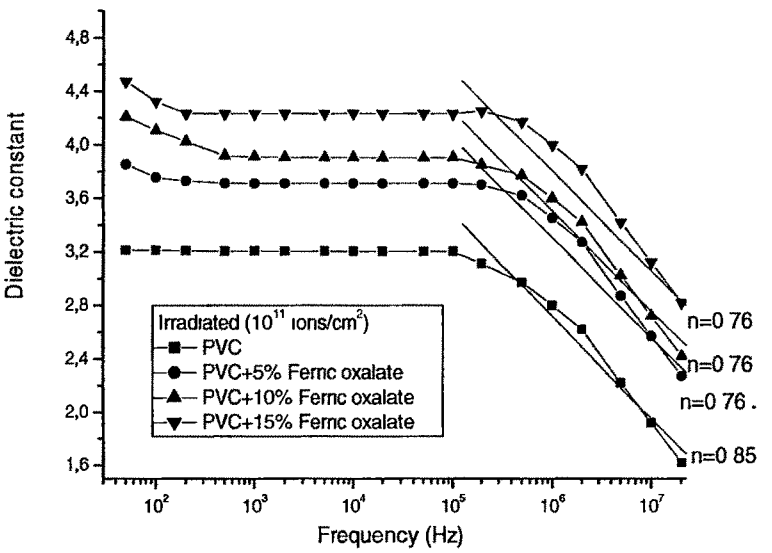

Figure 3.8(b) Plot of dielectric constant versus frequency for irradiated (at the fluence of1x 10^{11} ions/cm^2) pure and ferric oxalate dispersed compound in PVC films.

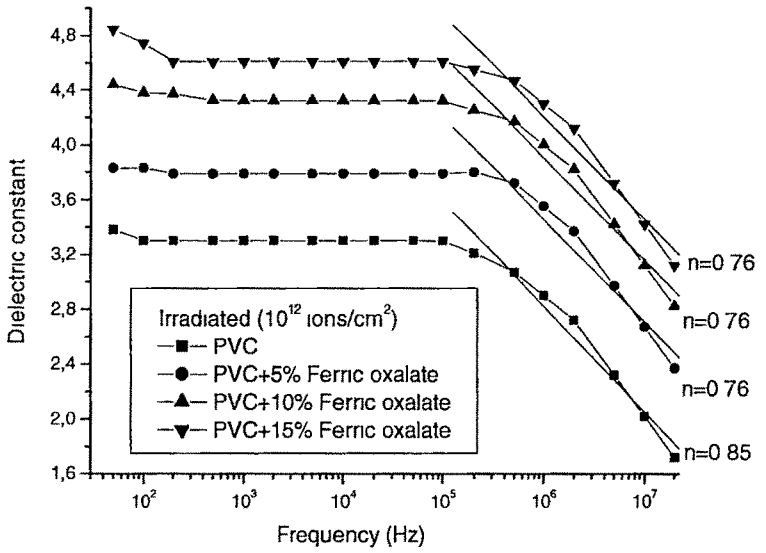

Figure 3.8(c) Plot of dielectric constant versus frequency for irradiated (at the fluence of 1x10^{12} ions/cm^2) pure and ferric oxalate dispersed compound in PVC films.

As evident from Fig 3.8, the dielectric constant remains almost constant up to 100 kHz. At these frequencies, the motion of free charge carriers is constant and so the dielectric constant presumably remains unchanged.

It is also observed that dielectric constant increases for irradiated films with the fluence.The increase in dielectric constant may be attributed to the chain scission and as a result the increase in the number of free radicals, etc. As frequency increases further (i.e. beyond 100 kHz), the charge carriers migrate through the dielectric and get trapped against a defect sites and induced an opposite charge in its vicinity. At these frequencies, the polarization of trapped and bound charges can not take place and hence the dielectric constant decreases [13]. The dielectric constant decreases at higher frequencies (i.e. beyond 100kHz) obeys the Universal law [14] of dielectric response given by $\varepsilon \alpha f^{n-1}$,

where n is power law exponent and varies form zero to one (0<n<1) , n=0.76 for pure PVC and 0.74 for all dispersed ferric oxalate pristine films. The value of n=0.85 for pure PVC and 0.76 for all dispersed ferric oxalate irradiated samples were obtained at the fluence of 1x 10^{11} ions/cm^2 (Fig.3.8b) and 1x 10^{12} ions/cm^2 (Fig.3.8c) respectively. The Fig. 3.8 (a, b and c) clearly shows that the frequency dependence of dielectric constant, ε, obeys Universal law. The observed nature of the fluence dependence of dielectric constant in studied frequency range can be explained by the prevailing influence of the enhanced free carriers due to the irradiation [15].

3.2.1 (c) Dielectric loss vs frequency

Fig.3.9 (a, b and c) shows the variation of dielectric loss with frequency for pristine and irradiated samples of pure PVC and ferric oxalate dispersed PVC films at the concentration of 5%,10% and 15% respectively. The dielectric loss decreases with increasing frequency. It is noticed that dielectric loss increases on increasing the concentration of filler and also with the fluence. The increase in the tanδ as the increase in the conductivity is brought about by an increase in the conduction of residual current and conduction of absorbance current [16].

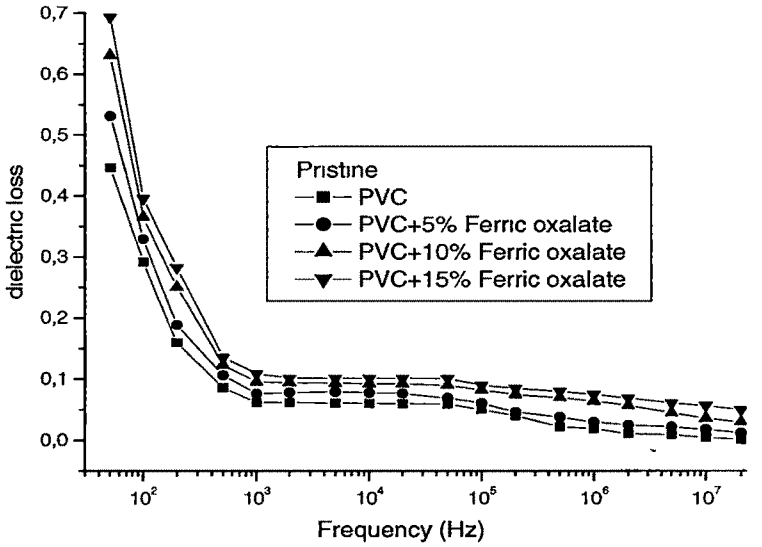

Figure 3.9(a) Plot of dielectric loss versus frequency for pristine pure and dispersed ferric oxalate compound in PVC films.

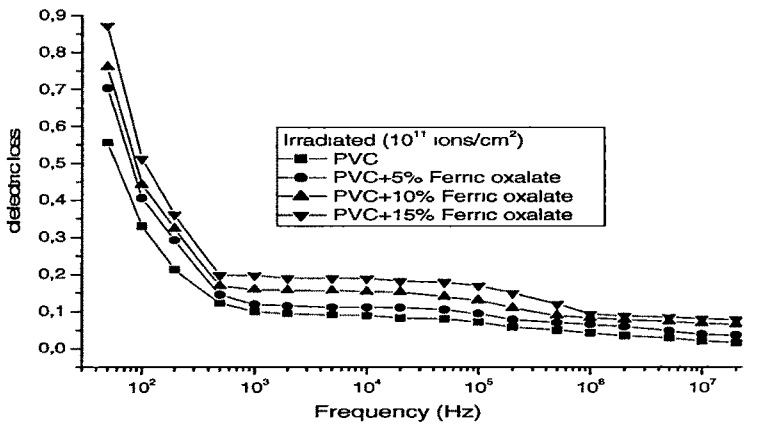

Figure 3.9(b) Plot of dielectric loss versus frequency for irradiated (at the fluence of 1x 10^{11} ions/cm^2) pure and ferric oxalate dispersed compound in PVC films.

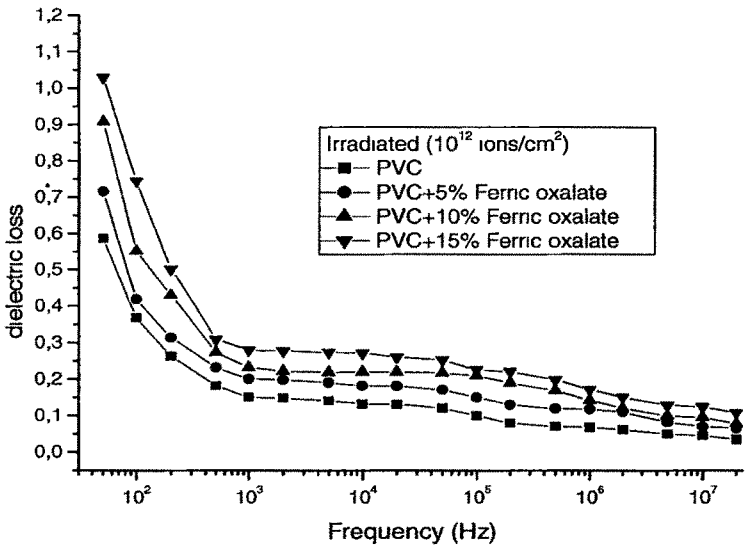

Figure 3.9(c) Plot of dielectric loss versus frequency for irradiated (at the fluence of 1x 10^{12} ions/cm^2) pure and ferric oxalate dispersed compound in PVC films.

3.2.2 Microhardness

The Vicker's microhardness was calculated using formula 2.10 given in article 2.4.2 Chapter 2. Fig.3.10(a, b and c) shows the plot of the Vickers' microhardness (H_v) versus applied load (P) for pristine and irradiated films of pure PVC, and dispersed ferric oxalate compound of 5%, 10% and 15% in PVC. The microhardness indentations were carried out on the surface of the pristine and irradiated films at room temperature under the different applied loads from 50 mN to 1000 mN and at a constant loading time of 30 seconds. It was observed that the microhardness (H_v) value increases with the load up to 100 mN and then decreases and become saturated beyond the load of 400 mN. Hardness can be defined as the resistance to indenter penetration, or as the average pressure under the indenter, calculated as the applied load divided by the projected area of contact

incorporating the plastic component of displacement. The hardness is known to be influenced by surface effects. At the higher loads, beyond 400 mN, the interior of the bulk specimen is devoid of surface effects. Hence the hardness value at higher loads represents the true value for the bulk and it is consequently independent of the load. Beyond the load of 400mN, the polymer exhausts its strain hardening capacity and hardness trends to become constant. The rate of strain hardening is greater at low loads and decreases at higher loads [17, 18]. It was found that hardness increases as ferric oxalate concentration increases. This may be due to the improvement in bonding properties [16]. The hardness of polymer composites also increases on irradiation with fluences of 1x 10^{11} ions/cm^2 and 1x 10^{12} ions/cm^2 respectively. This may be attributed to the growth of a hydrogen depleted carbon network which makes the polymer more harder [3].

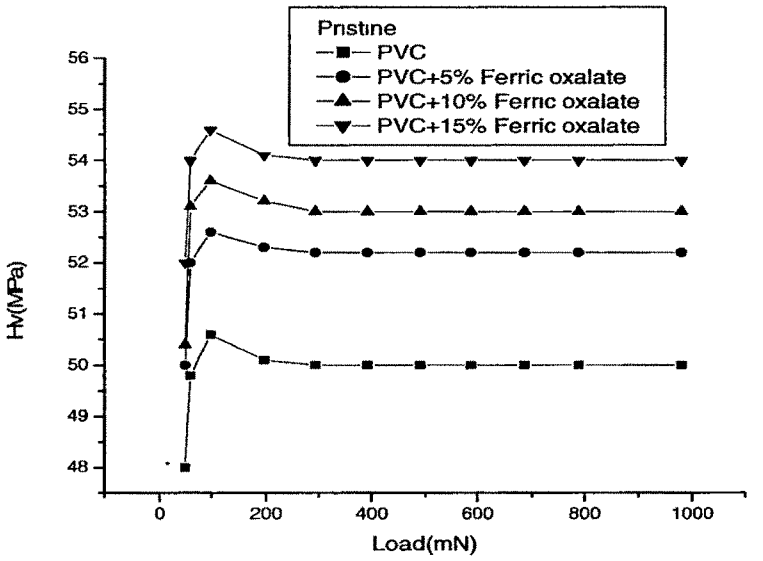

Figure 3.10(a) Plot of hardness (H_v) versus applied load (P) for pristine pure and dispersed Ferric oxalate compound in PVC films.

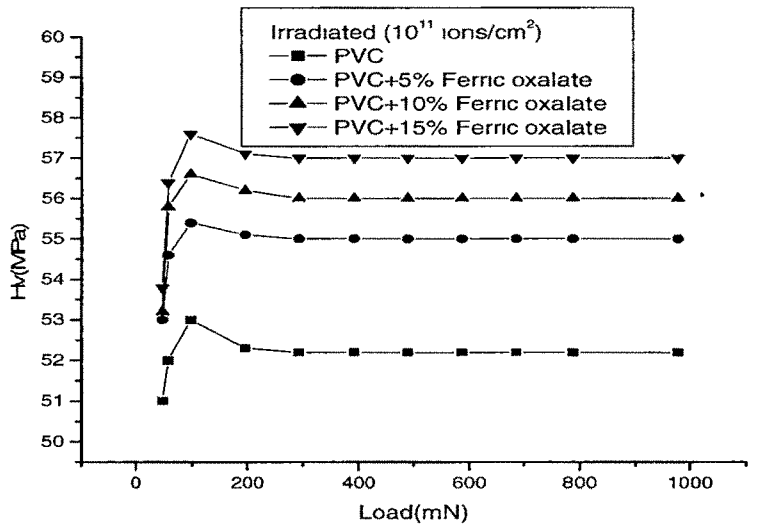

Figure 3.10(b) Plot of hardness (H_v) versus applied load (P) for irradiated (at the fluence of 1x 10^{11} ions/cm^2) pure and dispersed ferric oxalate compound in PVC films.

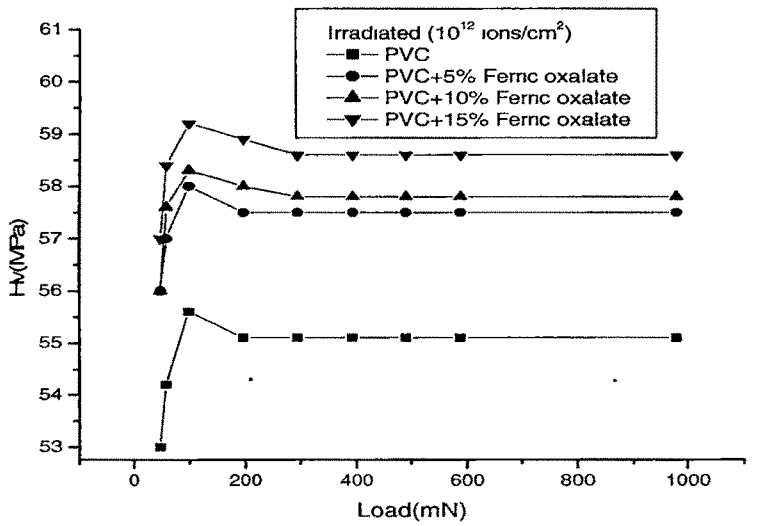

Figure 3.10(c)Plot of hardness (H_v) versus applied load (P) for irradiated (at the fluence of 1x 10^{12} ions/cm^2) pure and dispersed ferric oxalate compound in PVC films.

3.2.3 Surface Morphology

The surface morphology of pristine and irradiated samples was studied using AFM and SEM and discussed with respect to concentration of filler and ion fluence.The surface morphology of pristine and irradiated films of pure PVC, and dispersed ferric oxalate compound of 5% and 15% in PVC was measured by AFM on 5×5 μm^2 area as shown in Fig 3.11 Each AFM image was analyzed in terms of surface average roughness (Ra). The average roughness values are 5.7 nm, 9.3 nm, and 22 nm for unirradiated samples and those of irradiated samples the roughness values are 2.7 nm, 6.7 nm, 19.3nm at the fluence of 1x 10^{11} ions/cm^2 and 2.5nm, 5.4nm, 10.6nm at the fluence of 1x 10^{12} ions/cm^2 respectively.

It was found that roughness increases as ferric oxalate concentration increases. The increase in roughness may be due to the increase of density and size of metal particles on the surfaces of the PVC films [20]. It is also observed that after irradiation the roughness of the surface decreases and the surface becomes significantly smoother. This relative smoothness is probably due to defect enhanced surface diffusion [21, 22].

Fig.3.12 shows the surface morphology of composite films with 15% ferric oxalate dispersed pristine and irradiated samples at the fluences of 1x 10^{11} ions/cm^2 and 1x 10^{12} ions/cm^2 respectively. After irradiation partial agglomeration of fillers and flake-like structures could be seen in the micrographs of SEM.

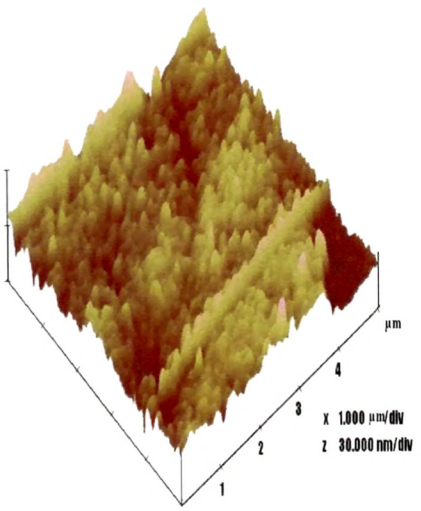

3.11(a)

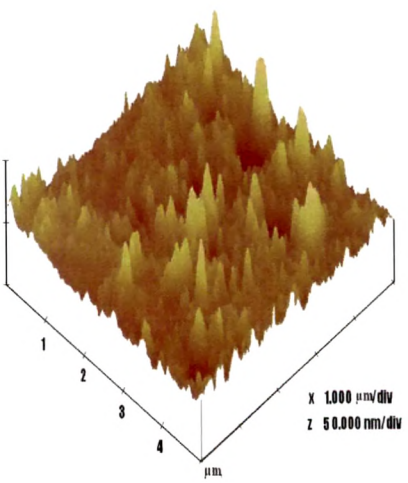

3.11(b)

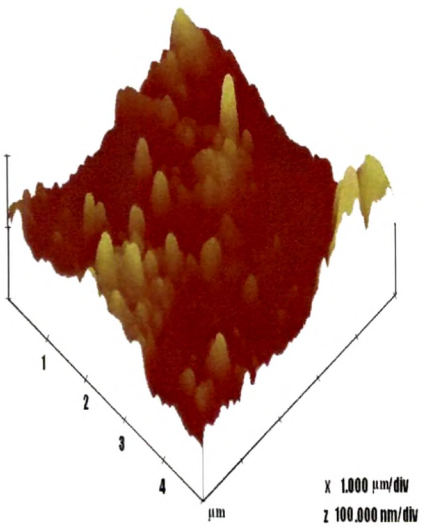

3.11(c)

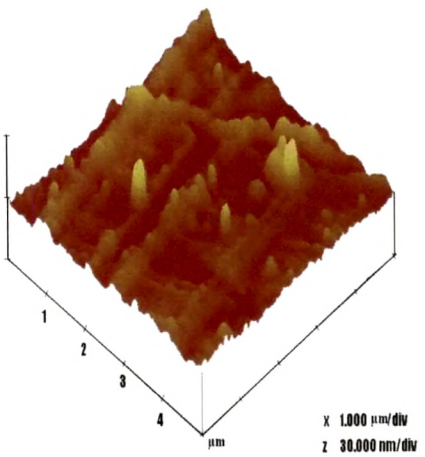

3.11(d)

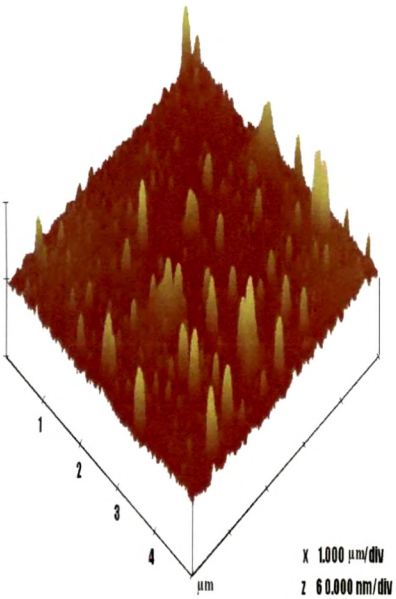

3.11(e)

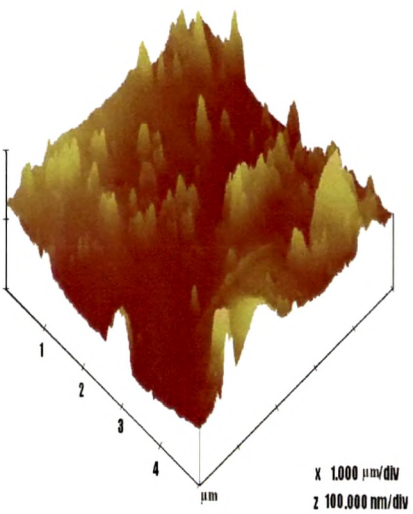

3.11(f)

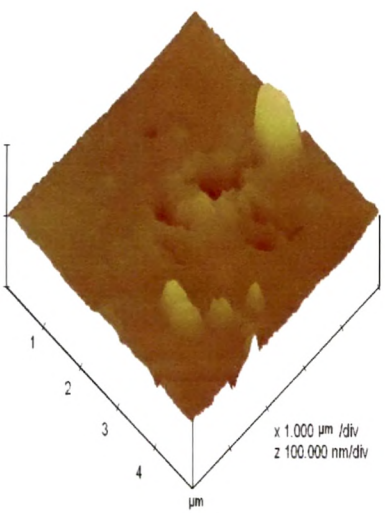

3.11(i)

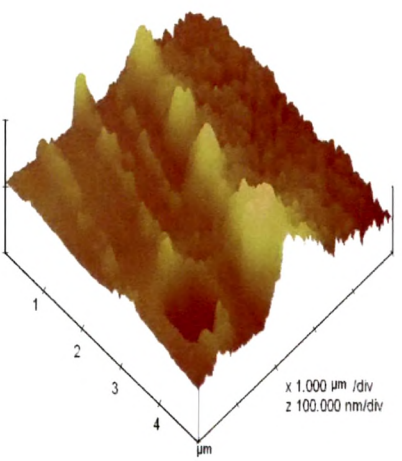

3.11(g)

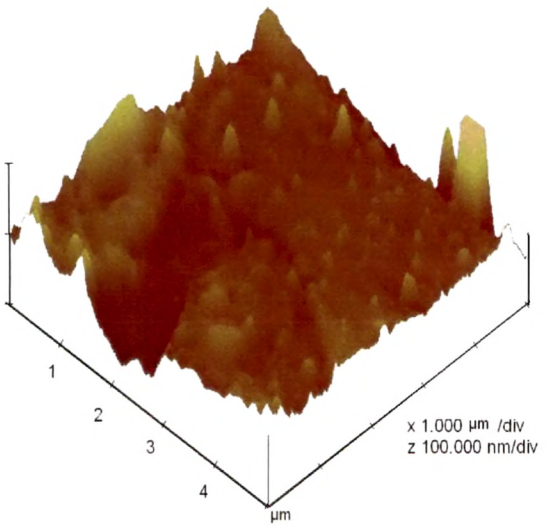

3.11(h)

Figure 3.11(a) AFM image of pure PVC film (pristine) (b) dispersed ferric oxalate (5%) in PVC film (pristine) (c) dispersed ferric oxalate (15%) in PVC film (pristine) (d) AFM image of pure PVC film (irradiated at the fluence of x 10^{11} ions/cm^2) (e) dispersed ferric oxalate (5%) in PVC film (irradiated at the fluence of 1x 10^{11} ions/cm^2) (f) AFM image of dispersed ferric oxalate (15%) in PVC film (irradiated at the fluence of 1x 10^{11} ions/cm^2) (g) AFM image of pure PVC film (irradiated at the fluence of x 10^{12} ions/cm^2) (h) AFM image of dispersed ferric oxalate (5%) in PVC film (irradiated at the fluence of 1x 10^{12} ions/cm^2) (i) AFM image of dispersed ferric oxalate (15%) in PVC film (irradiated at the fluence of 1x 10^{12} ions/cm^2).

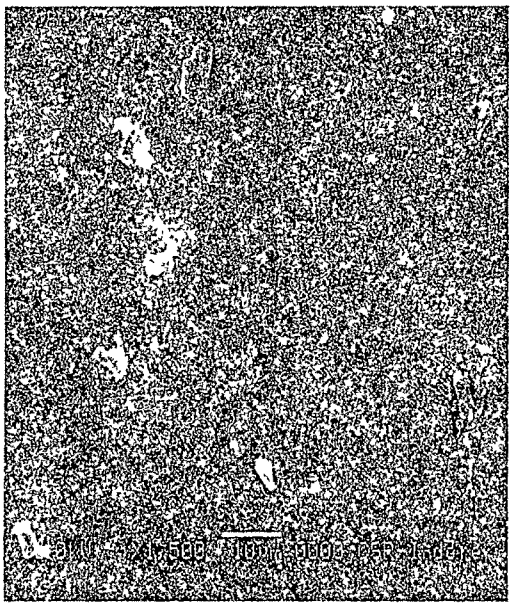

3.12(a)

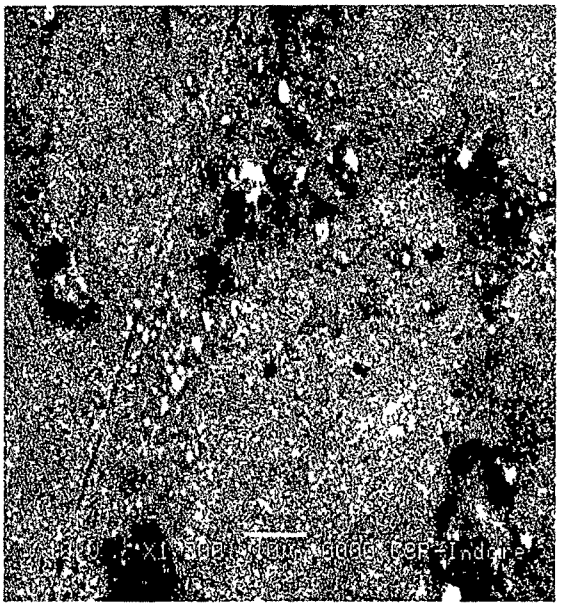

3.12 (b)

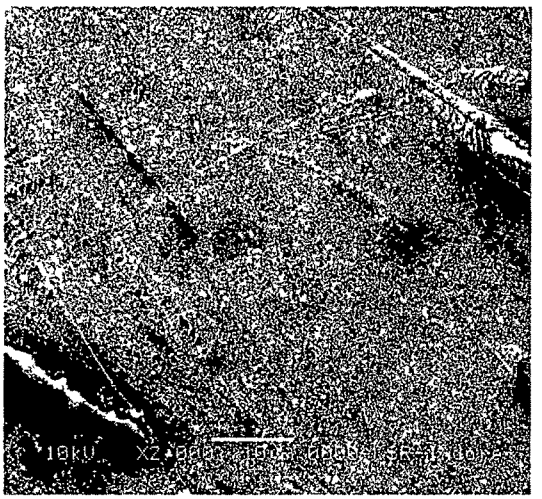

3.12 (c)

Figure 3.12 (a) SEM micrograph of dispersed ferric oxalate (15%) in PVC film (pristine) (b) SEM micrograph of dispersed ferric oxalate (15%) in PVC film (irradiated at the fluence of 1x 10^{11} ions/cm^2) (c) SEM micrograph of dispersed ferric oxalate (15%) in PVC film (irradiated at the fluence of 1x 10^{12} ions/cm^2).

3.2.4 Conclusion

Ion irradiation has been shown to significantly enhance both electrical and microhardness of organometallic compound dispersed PVC films. It may be attributed to (i) metal to polymer bonding and (ii) conversion of the polymeric structure in to hydrogen depleted carbon network. Thus irradiation makes the polymer harder, more conductive. Dielectric loss and constant are observed to change significantly with the fluence. This might be attributed to breakage of chemical bonds and resulting in the increase of free radicals, unsaturation etc. It is also observed that dielectric constant obeys Universal law of dielectric response. The surface roughness increases as ferric oxalate concentration increases and decreases on irradiation as observed from AFM studies. After irradiation partial agglomeration of filler and flake-like structures were observed in the micrographs of SEM.

3.3 Ni-DMG Dispersed PMMA Films

3.3 Results and Discussion

3.3.1 AC Electrical Frequency Response

3.3.1 (a) Condcutivity vs frequency

The conductivity was calculated using the relation $\sigma=t/R\ A$ ($\Omega^{-1}cm^{-1}$), where R is the resistance measured, A is the cross-sectional area of the electrode and t is the thickness of the polymeric film as discussed in article 2.4.1 of Chapter 2 and plotted with respect to frequency. Fig.3.13 shows the variation of conductivity with frequency for the pristine and irradiated samples at different Ni-DMG concentrations. A sharp increase in conductivity was observed around 100 kHz for dispersed pristine and irradiated samples. It was also observed that conductivity increases with increasing concentration of dispersed Ni-DMG (un-irradiated) compound (Fig.3.13(a)) as well as those irradiated at a fluence of 1×10^{11} ions/cm^2 (Fig. 3.13(b)). The increase in conductivity at different Ni-DMG concentrations for pristine samples may be attributed to the conductive phase formed by the dispersed Ni-DMG compound in a polymer matrix. It is known that electrical conductivity of such composites depends on the type and concentration of the dispersed compound [11, 12]. As a result the conductivity of dispersed films increases with increasing the concentration of Ni-DMG compound in the polymer matrix. It is also observed from Fig.3.13 (b) that after the irradiation the conductivity increases with increasing concentration of the dispersed compound. Irradiation is expected to promote the metal-to-polymer bonding and convert the polymeric structure in to hydrogen depleted carbon network. It is this carbon network that is believed to make the polymers more conductive [3].

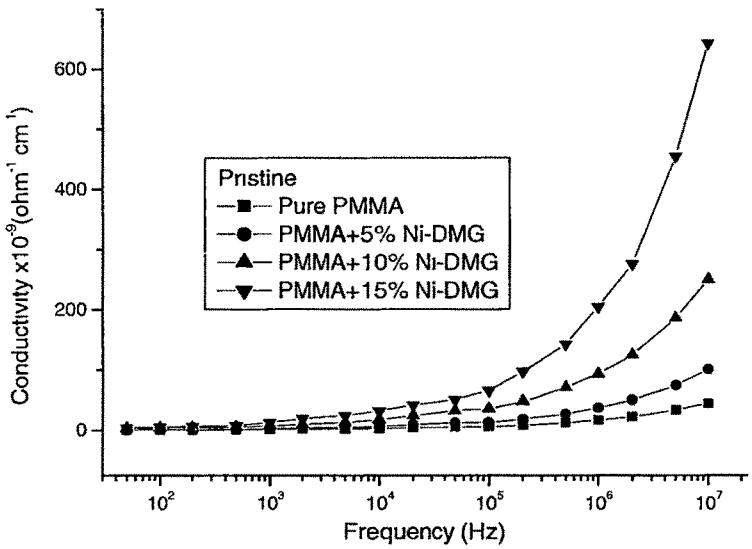

Figure 3.13(a) AC conductivity versus frequency for pristine pure and dispersed Ni-DMG compound in PMMA films.

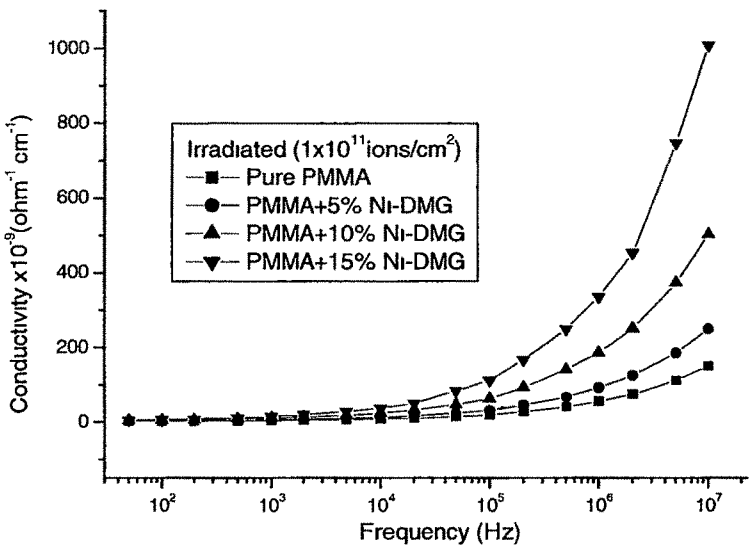

Figure 3.13(b) AC conductivity versus frequency for irradiated pure and dispersed Ni-DMG compound in PMMA films.

3.3.1 (b) Dielectric constant vs frequency

Dielectric constant was calculated using formula 2.8 as given in article 2.4.1 of Chapter 2. Fig 3.14 shows dielectric constant versus frequency for pristine and irradiated samples at different Ni-DMG concentrations. As evident from the graph, the dielectric constant remains almost constant up to 100 kHz. At these frequencies the mobility of the free charge carriers is constant and so the dielectric constant is constant. It is also evident that the dielectric constant increases as the Ni-DMG concentration increases for both pristine and irradiated samples.The magnitude of the dielectric constant is higher for irradiated films compared to that of pristine films. The increase in dielectric constant may be attributed to chain scission, which results in an increased abundance of free radicals, unsaturation, etc. As frequency increases further (i.e. beyond 100 kHz), the charge carriers migrate through the dielectric and get trapped against a defect sites and induced an opposite charge in its vicinity. At these frequencies, the polarization of trapped and bound charges can not take place and hence the dielectric constant decreases [13]. The dielectric constant decreases at higher frequencies (i.e. beyond 100 kHz) obeys the Universal law [14] of dielectric response given by $\varepsilon \alpha f^{n-1}$, where n is power law exponent and varies form zero to one ($0<n<1$), n=0.78 for pure PMMA, 0.84 for 5% Ni-DMG, 0.85 for 10%, and 0.87 for 15% Ni-DMG dispersed pristine films were observed respectively. The value of n=0.85 for pure PMMA, 5%, 10% and 15% dispersed Ni-DMG irradiated samples were obtained at the fluence of 1×10^{11} ions/cm^2 (Fig.3.14b). The Fig. 3.14 (a, b) clearly shows that the frequency dependence of dielectric constant, ε, obeys Universal law. The observed nature of the fluence dependence of dielectric

constant in studied frequency range can be explained by the prevailing influence of the enhanced free carriers due to the irradiation [15].

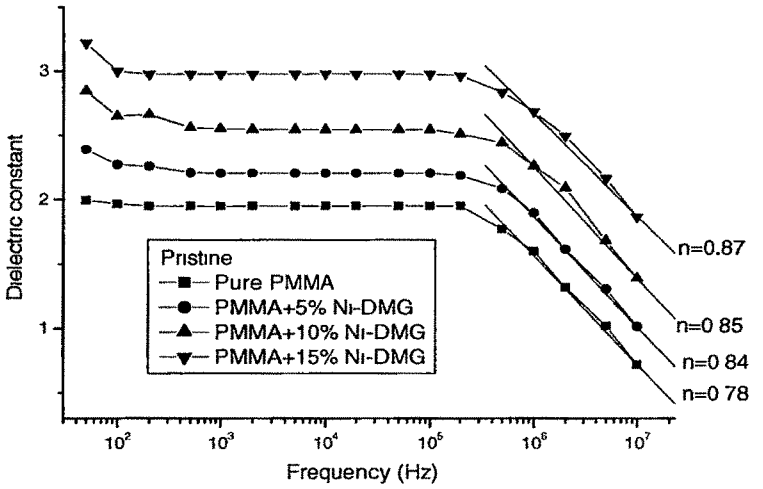

Figure 3.14(a) Dielectric constant versus frequency for pristine pure and dispersed Ni- DMG compound in PMMA films.

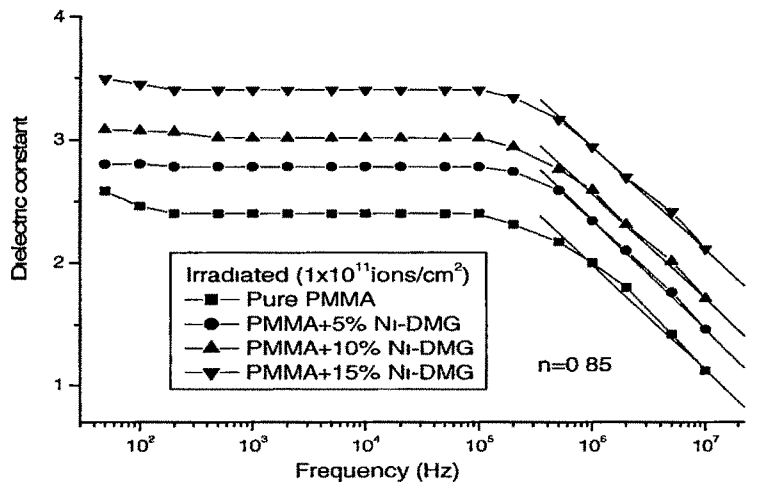

Figure 3.14(b) Dielectric constant versus frequency for irradiated pure and dispersed Ni-DMG compound in PMMA films.

3.3.1 (b) Dielectric loss vs frequency

Fig.3.15(a, b) shows the variation of dielectric loss with frequency for pristine and irradiated samples of pure PMMA and Ni-DMG dispersed PMMA films at the concentration of 5%, 10% and 15% respectively. The dielectric loss decreases sharply with increasing frequency. It is noticed that dielectric loss increases on increasing the concentration of filler and also with the fluence. The increase in the tanδ as the increase in the conductivity is brought about by an increase in the conduction of residual current and conduction of absorbance current [16].

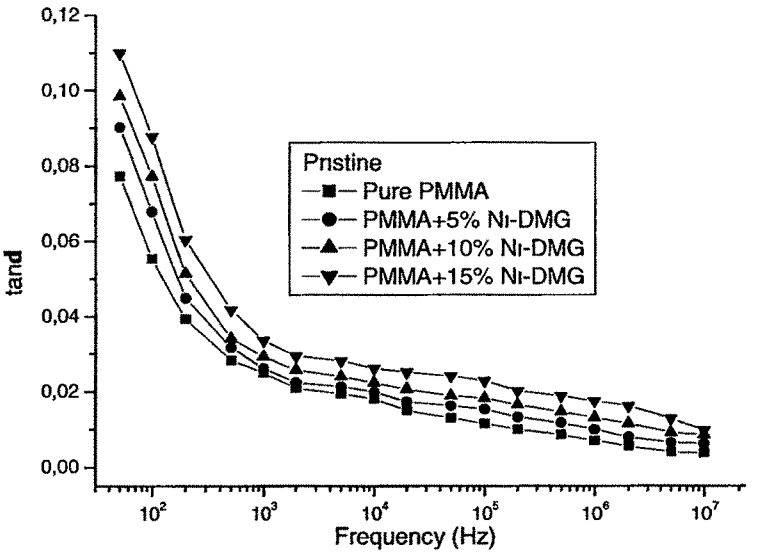

Figure 3.15(a) Dielectric loss versus frequency for pristine pure and dispersed Ni-DMG compound in PMMA films.

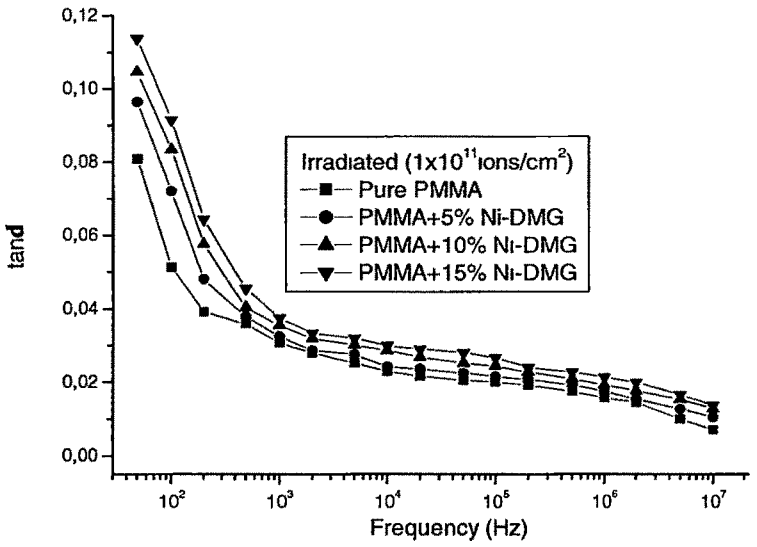

Figure 3.15(b) Plot of dielectric loss versus frequency for irradiated pure and dispersed Ni-DMG compound in PMMA films.

3.3.2 Microhardness

The Vicker's microhardness was calculated using formula 2.10 given in article 2.4.2 of Chapter 2. Fig.3.16 shows the plot of the Vickers' microhardness (H_v) versus applied load (P) for pristine (Fig.3.16 (a)) and irradiated (Fig.3.16 (b)) films of pure PMMA, and dispersed Ni-DMG compound of 5%, 10% and 15% in PMMA films. The microhardness indentations were carried out on the surface of the pristine and irradiated films at ambient temperature and at different loads from 50 mN to 1000 mN keeping constant loading time of 30 seconds. It was observed that the H_v value increases with the load up to 100 mN and then decreases and become saturated beyond the load of 400 mN. Hardness can be defined as the resistance to indenter penetration, or as the average pressure under the indenter, calculated as the applied load divided by the projected area

of contact incorporating the plastic component of displacement. The hardness is known to be influenced by surface effects. Particularly at low penetration depths, strain hardening modifies the true hardness of such material. At higher loads, beyond 400 mN, the interior of a bulk specimen is devoid of surface effects. Hence the hardness value at higher loads represents the true value for the bulk and it is consequently independent of the load.

It was found that hardness increases as Ni-DMG concentration increases. This may be due to the improvement in bonding properties [16]. The hardness also increases on irradiation of the samples. This may be attributed to the growth of a hydrogen depleted carbon network which makes the polymer harder [3].

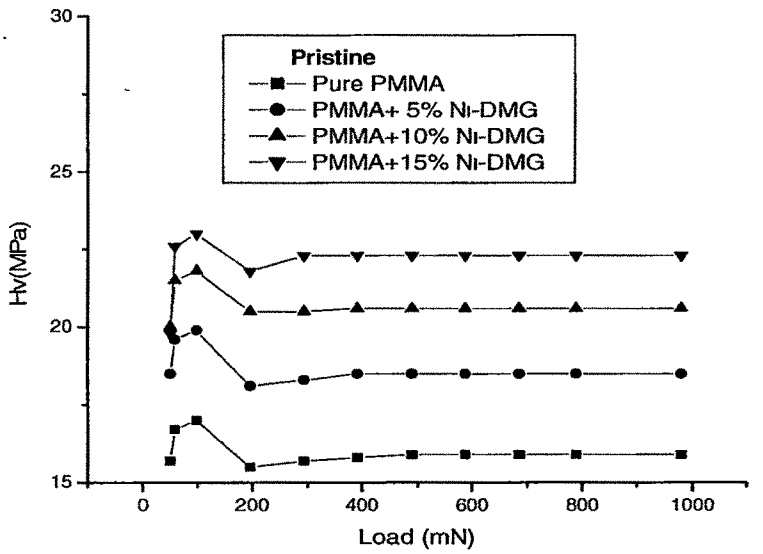

Figure 3.16(a) Plot of hardness (H_v) versus applied load (P) for pristinee pure and dispersed Ni-DMG compound in PMMA films.

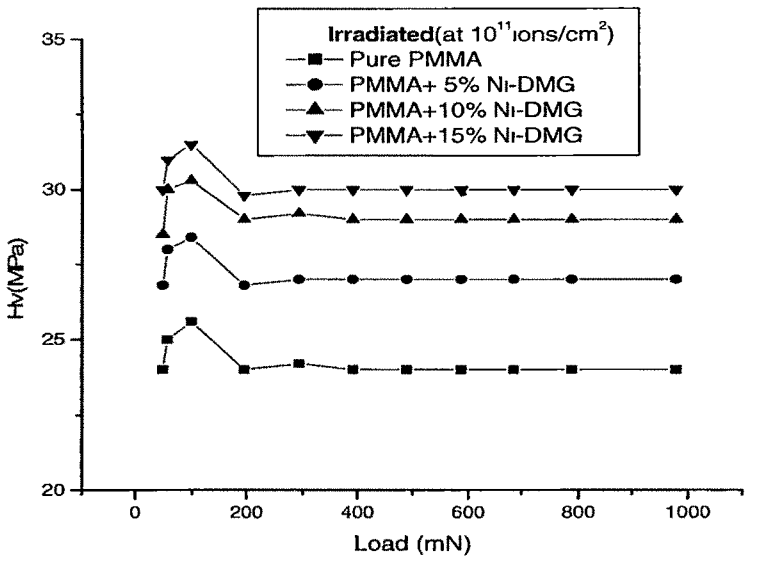

Figure 3.16(b) Plot of hardness (H_v) versus applied load (P) for irradiated pure and dispersed Ni-DMG compound in PMMA films.

3.3.3 Surface Morphology

The surface morphology of pristine and irradiated films of pure PMMA, and dispersed Ni-DMG compound of 10% and 15% in PMMA was measured by AFM on $2\times2\mu m^2$ area as shown in Fig.3.17. Each AFM image was analyzed in terms of surface average roughness (Ra). The roughness values are 13nm, 35.08nm and 83.59nm for pristine and 6nm, 21.66nm and 16.38nm for irradiated (at a fluences of 10^{11} ions/cm^2) samples respectively.

It was found that roughness increases as Ni-DMG concentration increases. The increase in roughness may be due to the increase of density and size of metal particles on the surfaces of the PMMA films [17]. It is also observed that after irradiation the

roughness of the surface decreases and the surface becomes significantly smoother. This relative smoothness is probably due to defect enhanced surface diffusion [21, 22].

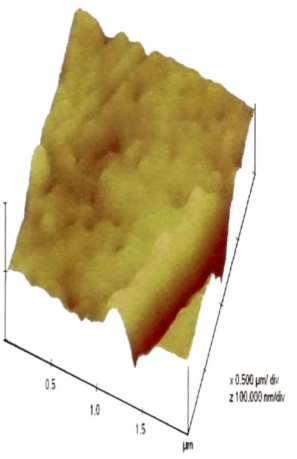

3.17(a)

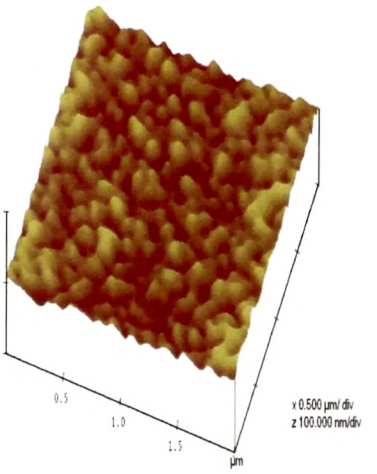

3.17(b)

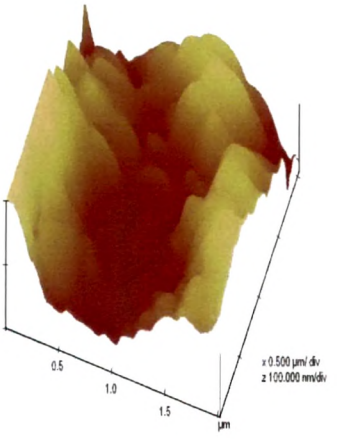

3.17(c)

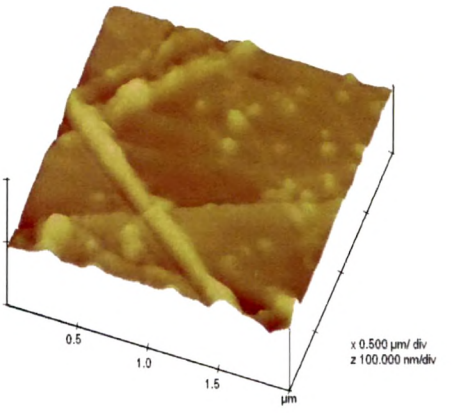

3.17(d)

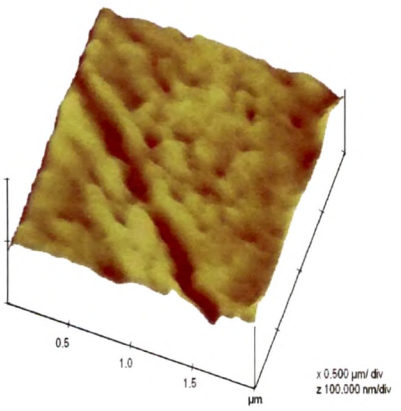

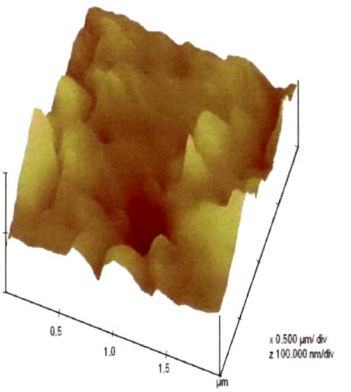

3.17(e) **3.17(f)**

Figure 3.17(a) AFM image of pure PMMA film (pristine) (b) dispersed Ni-DMG compound (10%) in PMMA film (pristine) (c) dispersed Ni-DMG compound (15%) in PMMA film (pristine) (d) pure PMMA film (irradiated) (e) dispersed Ni-DMG compound (10%) in PMMA film (irradiated) (f) dispersed Ni-DMG compound (15%) in PMMA film (irradiated).

3.3.4 Conclusion

Ion irradiation has been shown to significantly enhance both electrical and micro hardness of Ni-DMG compound dispersed PMMA films. It may be attributed to the metal-to-polymer bonding and conversion of the polymeric structure into hydrogen depleted carbon network. Thus irradiation makes the polymer harder and more conductive. It is also observed that dielectric constant obeys Universal law of dielectric response. The surface roughness increases as Ni-DMG concentration increases, but decreases on irradiation, as observed from AFM studies.

References

[1] S: Nowak, R Mauron, G. Dietler, and I. Schlapbch, in Metalized Plastics 2; Fundamental and Applied Aspects, edited By K. L. Mital (Plenum Press, New York, 1991)

[2] P. S. Ho, R. Height, R. C B. D. Silverman and F. Faupel, in: Fundamentals of Adhesion, edited by L. H. Lee, (Plenum Press, New York, 1991) p. 383.

[3] Y. Q. Wang, M. Curry, E. Tavenner, N. Dobson, R. E. Giedd Nucl.Instr. & Meth. **B 219-220** (2004)798.

[4] V. Zaporojtchenko, T. Strunskus, K. Behnke, C. von Bechtolsheim, M. Keine and F. Faupel, J. Adhesion Sci. Technol., **14** (2000)467.

[5] Anjum Qureshi, N. L. Singh, A. K. Rakshit, F. Singh, V. Ganesan, Nuclear Instruments and Methods **B 244** (2006) 235.

[6] Anjum Qureshi, N. L. Singh, A. K. Rakshit, D.K.Avasthi, V. Ganesan, Surface and Coatings Technology in press (2007).

[7] N. L. Singh, Anjum Qureshi, F. Singh and D. K. Avasthi, Material Science and Engineering **B 137**(2007)85.

[8] Anjum Qureshi, N. L. Singh, Keyur Somani, A. K. Rakshit, F. Singh, D.K.Avasthi, Indian Journal of Pure and Applied Physics **45** (2007)57.

[9] Anjum Qureshi, N. L. Singh, Keyur Somani, A. K. Rakshit, D. K. Avasthi, DAE Symposium on Solid State Physics **50C** (2005) 375.

[10] N. L. Singh, Anjum Qureshi, A. K. Rakshit and D. K. Avasthi, Bull. Mater. Sci. **29** (2006) 605.

[11] M. Abu-Abdeen, GM. Nasr, H. M. Osman and A. I. Abound. Egypt. J. Sol. **25**, (2002) 275.

[12] Ye. P. Mamunya, V. V. Davydenko, P. Pissis, E. V. Lebedev, European Polymer Journal **38** (2002)1887.

[13] A. K. Jonscher, Dielectric relaxation in solids. London: Chesla dielectric press; 1983.

[14] A. K. Jonscher, Nature, **267**(1977)673.

[15] T.Phukan, D. Kanjilal, T. D. Goswami, H. L. Das, Nucl Instr and Meth **B234** (2005) 520.

[16] N. P. Bogoroditsky, V. V. Pasynkov, B. M. Tareev, Electrical engineering materials, Mir Publisher, Moscow (1974).

[17] E. H. Lee, G. R. Rao, L. K. Mansur, Mater. Sci. Forum, **248-249** (1997)135.

[18] S. K. Awasthi and R. Bajpai, Indian Journal of Pure Applied Physics **39** (2001)795.

[19] W. H. Bowyer and M. G. Bader, J. Matt. Sci. 7 (1972) 1315.

[20] Xingbin Yan, Tao Xu, Shan Xu, Xiaobo Wang and Shengrong Yang, Nanotechnology, **15** (2004)1759.

[21] Yatendra S. Chaudhary, Saif A. Khan, Rohit Shrivastava, Vibha R. Satsangi, Satya Prakash, Umesh K. Tiwari, D. K. Avasthi, Navendu Goswami, Sahab Dass, Thin Solid Films **492** (2005)332.

[22] A. Biswas, D. K. Avasthi, D. Fink, J. Kanzow, U. Schurmann, S. J. Ding, O. C. Aktas, U. Saeed, V. Zaporojtchenko, F. Faupel, R. Gupta, N. Kumar, Nucl. Instr. and Meth. **B 217** (2004) 29.

[23] D. R. S. Somyajulu, C. N Murthy, D. K. Awasthi, N. V. Patel, and M. Sarkar Bull. Mater. Sci. **24** (2001)397.

[24] G. C. Psarras, E. Manolakaki, G. M.Tsangarris, Composites **A 33** (2001)375.

[25] A. E. Ghany, A. E. Salam, G. M. Nasr, J. Appl. Polym. Sci. **77**(2000)1816.